Cation Exchange in Lanthanide Fluoride Nanoparticles

Cunhai Dong and Frank C. J. M. van Veggel*

Department of Chemistry, the University of Victoria, P.O. Box 3065, Victoria, British Columbia, Canada V8W 3V6

ABSTRACT Cation exchange in lanthanide fluoride nanoparticles is reported. Typically, dispersible LnF_3 nanoparticles were exposed to another lanthanide ion that was roughly 5 times the amount of Ln^{3+} in the nanoparticles. Results show that cation exchange of GdF_3 nanoparticles with La^{3+} was almost complete in 1 min, and it also happens reversibly although the degree of exchange is not as much as the forward reaction. However, cation exchange with lanthanide ions close to each other, such as GdF_3 with Eu^{3+} and NdF_3 with La^{3+}, did not end up with nearly full exchange, but with a significant amount of the two lanthanides. A relatively small driving force for the cation exchange is suggested by the experimental results, which is also confirmed by calculations based on a thermodynamic cycle. This unprecedented finding in the field of lanthanide-based nanoparticles raises the question whether reported core−shell structures were indeed made and, at the same time, it opens up new pathways to make nanomaterials that cannot be made directly.

KEYWORDS: cation exchange · lanthanide fluoride · nanoparticles · thermodynamic cycle · core−shell

Cation exchange has been reported first on ionic semiconductor nanoparticles by Alivisatos.[1] It was demonstrated that cation-exchange reaction of Ag^+ with CdSe nanoparticles is reversible at room temperature although it is kinetically hindered at ambient conditions in the bulk. Following this, many different types of interesting functional nanomaterials, including hollow nanospheres of PbSe,[2] superlattices of CdS−Ag_2S on nanorods,[3] and nanowires of CdTe,[4] CdSe,[5] as well as core−shell nanoparticles of Se−Ag_2Se,[6] Se−CdSe,[6,7] Se−PbSe,[6] and PbSe−CdSe,[8] have been made in solution *via* cation-exchange reactions. So far, most of them cannot be synthesized directly.

Semiconductor nanomaterials have tunable, relatively broad emission and excitation peaks, but they suffer from photobleaching.[9] In contrast, lanthanide-based nanoparticles have non-overlapping, quite sharp excitation and emission peaks as well as very good photostability due to the shielded 4f orbitals by the filled 5s and 5p orbitals. These unique properties make lanthanide-based nanoparticles valuable in applications as biolabels,[10,11] photodynamic therapy,[12] optical amplifier in telecommunications,[13] and optical-display phosphors.[14,15] In addition, owing to seven unpaired 4f electrons, some nanoparticles of gadolinium salts have been reported for application as MRI contrast agents.[16−18] Among these lanthanide-based nanoparticles, lanthanide fluoride nanoparticles are receiving extensive attention because of their low phonon energies and thus minimum quenching of emissive Ln^{3+} ions, leading to suitable matrices for the optical applications.[19−22]

In comparison with the monovalent and bivalent ions in semiconductor nanomaterials, trivalent lanthanide ions have high hydration energies.[23] In addition, the diffusion of lanthanide ions in lanthanide fluorides is very likely to be inhibited due to the high lattice energies of lanthanide fluoride.[24] These two factors are expected to lead to higher activation energy for cation-exchange reaction in lanthanide fluorides as compared with the above-discussed semiconductor nanomaterials. It thus seems counter-intuitive that cation exchange in lanthanide fluoride nanoparticles would occur at ambient conditions. Nevertheless, we report here cation exchange in lanthanide fluoride nanoparticles in aqueous dispersions, which, to our knowledge, is unprecedented. A thermodynamic cycle is established to provide an explanation for the small driving force shown by the experimental results. We also discuss the implication for core−shell structures and the possibility to obtain nanomaterials that are otherwise inaccessible.

*Address correspondence to fvv@uvic.ca.

Received for review July 28, 2008 and accepted December 02, 2008.

Published online December 12, 2008.
10.1021/nn8004747 CCC: $40.75

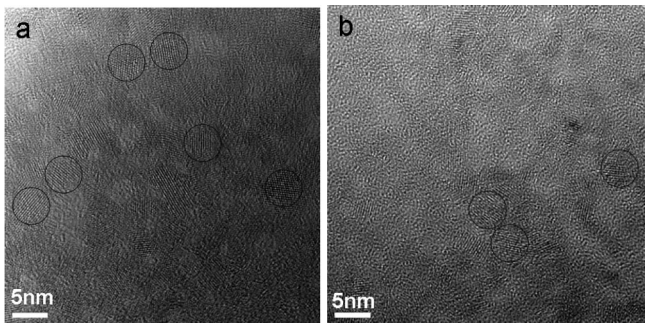

Figure 1. HR-TEM images of GdF_3 nanoparticles (a) before and (b) after cation exchange with La^{3+} (circles of 5 nm in diameter are used to highlight a few nanoparticles).

RESULTS AND DISCUSSION

Citrate-stabilized GdF_3 nanoparticles with a high water dispersibility were first prepared using a previously reported procedure.[24] These GdF_3 nanoparticles were then mixed with La^{3+} in the presence of extra citrate in an aqueous solution. The amount of La^{3+} used is roughly 5 times that of the Gd^{3+} in GdF_3 nanoparticles. It turned out that some extra citrate was needed to facilitate the reaction because without it nanoparticles precipitated. A possible reason for the precipitation is that the added La^{3+} ions extract a portion of the citrate ligand from the surface of nanoparticles. Without a sufficient amount of stabilizing ligand, the nanoparticles aggregate and precipitate from solution. After about 1 min reaction, nanoparticles were isolated with the same high water dispersibility as the as-prepared GdF_3 nanoparticles. High-resolution transmission electron microscopy (HR-TEM) images show that they are crystalline with sizes in the range of 5 nm before and after the cation exchange (Figure 1). The spacing of lattice fringes of GdF_3 nanoparticles is 3.20 Å, which is consistent with the *d* spacing of the (111) plane. Cation-exchanged nanoparticles have a spacing of 3.26 Å, which is consistent with the *d* spacing of the (111) plane of LaF_3. Energy dispersive X-ray (EDX) spectroscopy showed a La/Gd ratio of 11.04, indicating that 92% Gd^{3+} in GdF_3 nanoparticles had been replaced by La^{3+} (Table 1 and Figure S1a in the Supporting Information). X-ray diffraction (XRD) patterns show an obvious

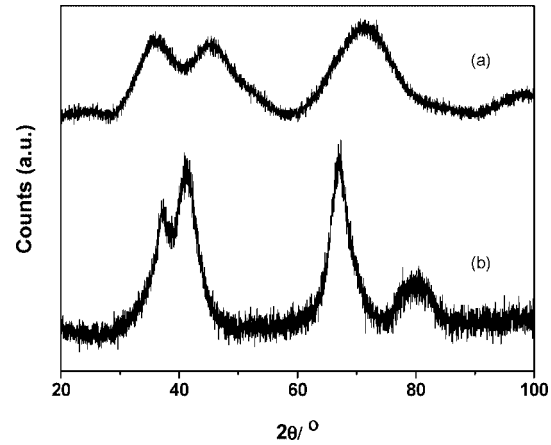

Figure 2. XRD patterns of (a) the as-prepared GdF_3 nanoparticles and (b) LaF_3 nanoparticles made by cation exchange of GdF_3 nanoparticles with La^{3+}.

change of diffraction pattern before and after the cation exchange (Figure 2). In another article by us, we showed that the GdF_3 nanoparticles of roughly 5 nm in size are not amorphous but that they are a mixture of both orthorhombic and trigonal phases, leading effectively to severely broadened XRD patterns, whereas LaF_3 nanoparticles have a single trigonal phase.[24] In fact, the pattern of the cation-exchanged nanoparticles is the same as the as-prepared LaF_3 nanoparticles, indicating that the crystal phase of GdF_3 nanoparticles had been transformed to that of LaF_3. Using Scherrer equation,[25] the crystallite size of LaF_3 nanoparticles prepared by cation exchange of GdF_3 nanoparticles with La^{3+} was estimated to be 4.2 nm, which is consistent with the size from TEM images.

The extra citrate used to facilitate the cation exchange does not disassemble nanoparticles. As a matter of fact, a large excess amount of citrate is always used for the synthesis of nanoparticles.[24] If the extra citrate disassembles nanoparticles, the complex of citrate−Ln^{3+} was produced, and thus nanoparticles would not be obtained. This is obviously not the case based on this and our previous work.[14,16,24] This was also verified by a simple experiment, in which citrate was mixed with the as-prepared GdF_3 nanoparticles in

TABLE 1. Summary of EDX Results of Cation-Exchanged Nanoparticles as Ln Ratios with Standard Deviation[a]

	GdF_3 with La^{3+}		LaF_3 with Gd^{3+}
	at 1 min	at 30 min	at 30 min
La/Gd ratio	11.04 ± 0.79	16.22 ± 0.76	3.58 ± 0.04
	EuF_3 with La^{3+} at 30 min	LaF_3 with Eu^{3+} at 30 min	
La/Eu ratio	19.45 ± 1.89	3.86 ± 0.17	
		NdF_3 with La^{3+} at 30 min	
La/Nd ratio		1.75 ± 0.01	
		GdF_3 with Eu^{3+} at 30 min	
Eu/Gd ratio		4.32 ± 0.10	
	$Na_{0.446}Yb_{0.554}F_{2.108}$ with La^{3+} at 30 min		LaF_3 with Yb^{3+} at 30 min
La/Yb ratio	18.62 ± 1.34		3.39 ± 0.05

[a]Standard deviations were calculated based on the three measurements on different spots of the sample.

an aqueous solution in the same ratio as used for the cation-exchange reactions. From the mixture, nanoparticles were isolated in the standard way. The isolated nanoparticles, as shown by XRD, display an identical diffraction pattern as the as-prepared GdF_3 nanoparticles (Figure 3), evidencing that there is no size change when nanoparticles were exposed to the solution of citrate.

The mass balance of cation exchange was verified by a reaction of exposing 2.5% Eu^{3+}-doped GdF_3 nanoparticles to La^{3+} for a minute. Because the La^{3+} ions used were in excess (roughly 5 times the amount of Gd^{3+} ion in GdF_3 nanoparticles), the majority of La^{3+} ions, along with the replaced Gd^{3+} ions, should remain in the reaction mixture as complexes formed with extra citrate or as free ions. Once ethanol was added to precipitate the cation-exchanged nanoparticles from solution by centrifuge, complexes and free ions ended up in the supernatant while nanoparticles stayed in the bottom of centrifuge tubes. The supernatant was rotovaped to dryness. EDX was done on both cation-exchanged nanoparticles and dried supernatant. The content of Eu is beyond the detection limit of EDX for both. A La/Gd ratio of 12.76 was obtained for nanoparticles (Figure S2a in the Supporting Information), indicating that 93% of Gd^{3+} and Eu^{3+} had been replaced by La^{3+}, which is almost the same as the results of cation exchange for the undoped GdF_3 nanoparticles. A La/Gd ratio of 4.78 was obtained for the supernatant (Figure S2b in the Supporting Information). This is consistent with the reaction condition that the amount of La^{3+} ion added is roughly 5 times that of Gd^{3+} and Eu^{3+} ions in the GdF_3 nanoparticles. In order to provide a clearer picture about cation exchange reaction, Eu^{3+} dopant is used as probe to verify the cation-exchange reaction and to show in what form Gd^{3+} and Eu^{3+} ended up in the supernatant because the luminescence of Eu^{3+} is sensitive to its environment.[25] The effective lifetimes (see the detailed method in Experimental Section) of Eu^{3+} emission in the as-prepared GdF_3 nanoparticles, cation-exchanged nanoparticles, and supernatant were measured to be 1.70, 4.20, and 0.34 ms, with an estimated error of $\pm 5\%$ (Figure 4). The increase in the lifetime from the as-prepared GdF_3 nanoparticles to cation-exchanged nanoparticles is due to two reasons. One is the reduction of concentration of Eu^{3+} in nanoparticles by cation exchange, which reduces concentration quenching. The other reason is that the point symmetry of Eu^{3+} in GdF_3 (C_s) is slightly less than that in LaF_3 (C_2),[26] leading to a shorter lifetime. In sharp contrast, the lifetime of Eu^{3+} emission in supernatant is much shorter than that in the two nanoparticles. This confirms that the Eu^{3+} in the supernatant is in the form of complex and/or solvation, which results in significant quenching of the Eu^{3+} emission, leading to a short lifetime. From the decay curve of Figure 4c, a very small amount of long-lived components can be seen. This could be from a minor amount of nanoparticles still dispersed in the supernatant after precipitation by ethanol. The method we used to calculate the effective lifetime includes the counts down to 1% of the initial counts. Hence, for the lifetime calculation of the Eu^{3+} emission in the supernatant, the minor amount of long-lived components was not included. From the above luminescence results of Eu^{3+}, it can be concluded that the excess La^{3+} and the replaced Ln^{3+} ions ended up in the supernatant as complexes or free ions.

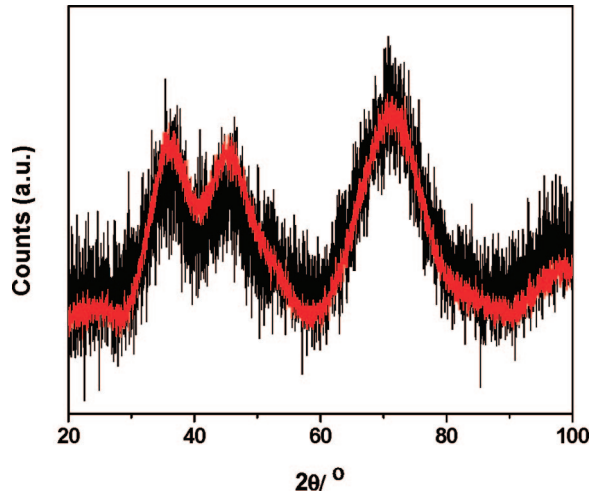

Figure 3. XRD patterns of the as-prepared GdF_3 nanoparticles (in red) and the citrate-treated GdF_3 nanoparticles (in black).

In order to investigate the kinetics of the cation-exchange reaction of GdF_3 nanoparticles with La^{3+}, the cation-exchanged nanoparticles were isolated at 1 and 30 min, respectively. EDX results show that the nanoparticles isolated at 1 min have only 8% Gd^{3+} left. However, at 30 min, there is 6% Gd^{3+} left (Table 1). These suggest that, upon mixing, the rate of cation exchange was very fast (*i.e.*, nearly complete in the first minute). After that, cation exchange was still in progress.

The reversibility of cation exchange was checked by exposing LaF_3 nanoparticles to Gd^{3+} under other-

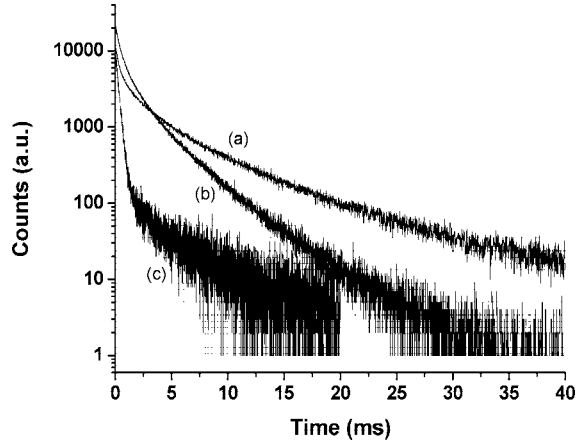

Figure 4. Decay curves of the Eu^{3+} $^5D_0$ level in (a) the exchanged nanoparticles, (b) the as-prepared GdF_3 nanoparticles, and (c) the supernatant.

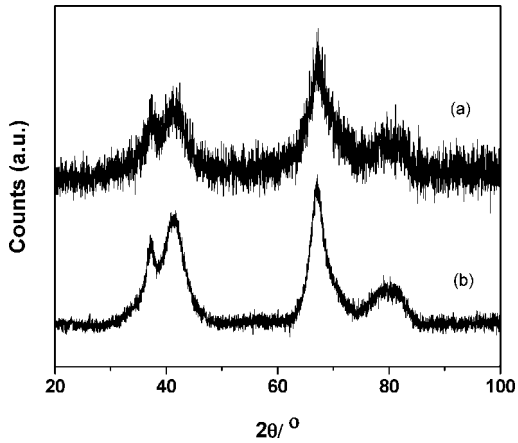

Figure 5. XRD patterns of (a) LaF_3 nanoparticles after exposed to Gd^{3+} and (b) the as-prepared LaF_3.

wise identical conditions. After 30 min, the cation-exchanged nanoparticles have a La/Gd ratio of 3.58 (Table 1 and Figure S1b in the Supporting Information), that is, 22% La^{3+} had been replaced by Gd^{3+} although the crystal phase remains the same as the as-prepared LaF_3 nanoparticles (Figure 5). Therefore, cation exchange can indeed take place reversibly albeit with different extents of exchange.

It is counter-intuitive that such fast cation-exchange reactions occur. In principle, cation exchange can take place through solution because of the finite solubility of LnF_3 and hence the difference in solubility product (K_{sp}) could lead to some exchange. Although the data of K_{sp} are only available for YF_3 and ScF_3, K_{sp} can be calculated for all the LnF_3. The calculated K_{sp} values of YF_3 and ScF_3 (1.16×10^{-20} and 1.09×10^{-23}, respectively) are within a factor of 2 of the experimental data (8.62×10^{-21} and 5.81×10^{-24}, respectively;[27] see Supporting Information for details), which lends confidence to the appropriation of the calculation. It turned out that K_{sp} of LaF_3 (4.26×10^{-19}) is much higher than that of GdF_3 (4.30×10^{-23}). This higher K_{sp} of LaF_3 favors precipitation of GdF_3. Therefore, if cation exchange takes place through solution due to the difference in K_{sp}, the nanoparticles isolated after cation exchange should be GdF_3. This is opposite to the experimental results, indicating that cation exchange is not accomplished through solution; therefore, it must be through the diffusion of ions in the LnF_3 nanoparticles as a solid state reaction. In fact, cation exchange in semiconductor nanoparticles was reported much faster (milliseconds[28]) than that in the bulk (minutes[29]). To our best knowledge, the only data available for LnF_3 are the diffusion coefficients of La^{3+} in LaF_3 nanoclusters at high temperatures. The lowest temperature reported is 530 K, at which the diffusion coefficient of La^{3+} is around 1×10^{-11} cm^2/s.[30] Consequently, the time it takes for La^{3+} to diffuse a diffusion length of 5 nm was calculated with the equation $L_D = \sqrt{4Dt}$ to be 6 ms. The temperature used in our cation exchange reaction was 350 K, lower than the lowest temperature at which diffusion coefficient is available in the literature. The diffusion coefficient decreases as the temperature decreases. However, for LaF_3 nanoclusters, the diffusion coefficients at 880 and 1690 K are around 3×10^{-11} and 1×10^{-9} cm^2/s, respectively.[30] Even if the diffusion coefficient drops from 1×10^{-11} to 1×10^{-13} cm^2/s, due to the decrease in temperature from 530 to 350 K, it takes less than 1 s to achieve a diffusion length of 5 nm. Therefore, it is reasonable to expect, in principle, a complete exchange in a minute. Although the exact mechanism of cation exchange is not known, it could occur by a hopping mechanism through Ln^{3+} vacancies. The fact that cation exchange happens more readily in nanoparticles than in bulk suggests that a much larger number of vacancies might exist. This would be consistent with the lower reaction temperature for these dispersible nanoparticles compared to many bulk preparations that involve high-temperature annealing steps.

The generality of cation exchange in lanthanide fluoride nanoparticles was also demonstrated with different lanthanide ions. Reaction of EuF_3 with La^{3+} gives a La/Eu ratio of 19.45, and the reverse reaction gives a La/Eu ratio of 3.86 (Table 1). These results are very similar to those of reactions of GdF_3 with La^{3+}, which is consistent with the fact that gadolinium and europium are next to each other in the periodic table of elements, and thus their sizes and chemical properties are very similar. Therefore, for the neighboring lanthanides, cation exchange should result in a mixture rather than nearly complete exchange. In fact, a reaction of NdF_3 with La^{3+} indeed produced a mixture with La/Nd ratio of 1.75. Similarly, a reaction of GdF_3 with Eu^{3+} produced a mixture with Eu/Gd ratio of 4.32 (Table 1). Cation exchange was also studied with previously prepared $Na_{0.446}Yb_{0.554}F_{2.108}$ nanoparticles[24] by mixing with La^{3+}. After cation exchange, the cubic crystal phase of $Na_{0.446}Yb_{0.554}F_{2.108}$ nanoparticles had been transformed to the trigonal phase of LaF_3 (Figure 6) with a La/Yb ratio of 18.62 (Table 1). A balanced reaction equation for this cation exchange is presented for a stoichiometric phase:

$$NaYbF_4 + 4/3La^{3+} \rightarrow 4/3LaF_3 + Na^+ + Yb^{3+}$$

However, the crystal phase of LaF_3 nanoparticles remains the same after exposed to Yb^{3+} (Figure 7) with a La/Yb ratio of 3.39 (Table 1). From these experimental results, we can also see a trend that the early lanthanide ions replace the late lanthanide ions in lanthanide fluoride nanoparticles with a relatively high extent of exchange as compared with the reverse.

The above results show that cation-exchange reaction takes place reversibly albeit with a different extent of exchange. That is to say, the cation-exchange reaction has a relatively small driving force (*i.e.*, Gibbs free

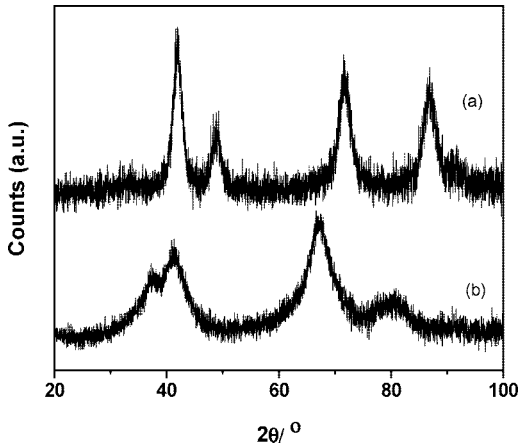

Figure 6. XRD patterns of (a) the as-prepared $Na_{0.446}Yb_{0.554}F_{2.108}$ nanoparticles and (b) LaF_3 nanoparticles made by cation exchange of $Na_{0.446}Yb_{0.554}F_{2.108}$ nanoparticles with La^{3+}.

energy of the forward reaction of GdF_3 with La^{3+} is only slightly negative). In order to calculate the driving force of the cation-exchange reaction, the following thermodynamic cycle was established with the reaction of GdF_3 with La^{3+} used as an example (Figure 8). The hydration energy of F^- is −472 kJ/mol, that of La^{3+} −3155 kJ/mol, and that of Gd^{3+} −3385 kJ/mol.[23] Lattice energies and entropy changes of the lanthanide fluorides were taken from another article by us.[24] Binding constants between citrate and the Ln^{3+} ions are of the same order of magnitude,[31] and thus, the free energy associated with the citrate−Ln^{3+} interactions cancels. According to the Debye−Hückel law, the activity coefficient is the same for Gd^{3+} and La^{3+} because cation exchange does not change the ionic strength. Therefore, the deviations from ideality are the same and thus cancel each other. In addition, because of the similar binding constants between surface citrate and Ln^{3+} ions and the similar sizes of nanoparticles before and after cation exchange, we assume that the number of citrate molecules on the surface of nanoparticles is the same, so this contribution also cancels. For the same

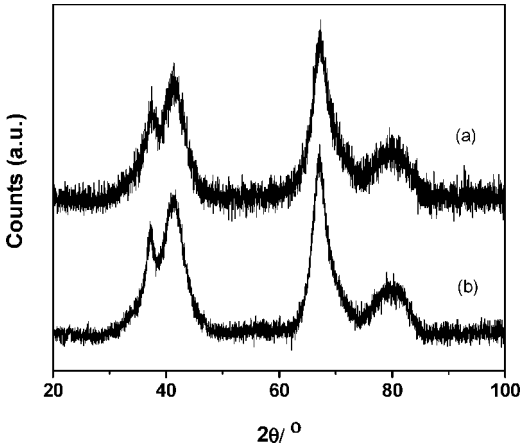

Figure 7. XRD patterns of (a) LaF_3 nanoparticles after exposed to Yb^{3+} and (b) the as-prepared LaF_3.

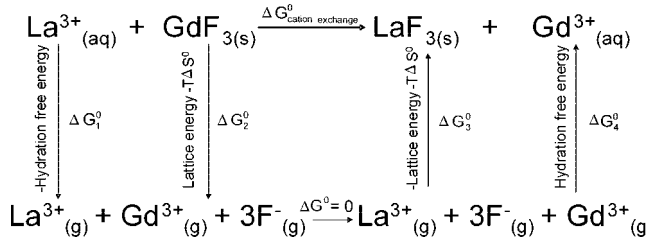

Figure 8. Thermodynamic cycle of the cation-exchange reaction.

reason, the changes of hydration energy of Ln^{3+} ions due to the interaction with citrate are assumed to be of the same order of magnitude, as well. Another factor that should be considered is surface free energies of nanoparticles. However, the sizes of these roughly spherical nanoparticles are nearly the same before and after cation exchange, and their compressibilities are expected to be of the same order of magnitude. Moreover, the difference in lattice energies is within 5%.[24] Therefore, it is reasonable to assume the same surface free energies for nanoparticles before and after cation exchange.

$\Delta G^0_{\text{cation exchange}}$ was calculated to be 29 kJ/mol for the forward reaction of GdF_3 with La^{3+}, which is different than the small negative value shown by the experimental results. However, the value is around 1% when compared to the lattice energies and the hydration energies in the thermodynamic cycle. In fact, the errors in the lattice energies[24] and the hydration energies[23] are in the range of 0.5−2%. Hence, a small difference in the lattice energies or/and the hydration energies would change the sign of $\Delta G^0_{\text{cation exchange}}$. This is confirmed by the same calculations carried out for the reaction of NdF_3 with La^{3+} and for the reaction of GdF_3 with Eu^{3+}, which give $\Delta G^0_{\text{cation exchange}}$ of −6 and −20 kJ/mol, respectively (due to the lack of the fundamental data, calculations cannot be done for $Na_{0.446}Yb_{0.554}F_{2.108}$). In any case, the calculated values of $\Delta G^0_{\text{cation exchange}}$ are close to zero, which is consistent with the small driving force shown by the experimental results. As a matter of fact, as the atomic number of lanthanide increases from La to Lu, the hydration energy of lanthanide ion becomes more negative,[23] while the lattice energy of lanthanide fluoride becomes more positive.[24] For instance, in the above thermodynamic cycle, the hydration energy of La^{3+} is less negative than that of Gd^{3+}, whereas the lattice energy of GdF_3 is more positive than that of LaF_3 (the term $T\Delta S^0$ is nearly the same for GdF_3 and LaF_3, 152 and 150 kJ/mol, respectively[24]). These energy differences are of the same magnitude. Thus, the free energy gain in the hydration energy from La^{3+} to Gd^{3+} is the energy loss in the lattice energy from GdF_3 to LaF_3. As a result, the overall Gibbs free energy of cation-exchange reactions should be close to zero, as indeed observed by us.

As demonstrated above, cation exchange takes place when lanthanide fluoride nanoparticles are ex-

posed to another Ln^{3+} ion. Similarly, core−shell nanoparticles are generally prepared by exposing core nanoparticles to the respective ions of the shell, and assumingly, the shell grows on the core particles epitaxially. Generally, there are two ways to add the respective ions of the shell. One way is to add Ln^{3+} first and then F^-. For example, in the literature, EuF_3 nanoparticles were exposed to Gd^{3+} followed by the addition of F^- to make EuF_3−GdF_3 core−shell nanoparticles;[32] CeF_3 nanoparticles were exposed to La^{3+} followed by the addition of F^- to make CeF_3−LaF_3 core−shell nanoparticles.[33] However, cation exchange, as shown by our results, is very likely to have happened. The chemical composition of the core nanoparticles could thus have been changed due to the cation exchange before the formation of the core−shell architecture. Consequently, the final nanoparticles may not have a true core−shell structure, but probably a gradient of two lanthanide fluorides. The other way to add the respective ions of the shell is to add F^- first and then Ln^{3+}. In this case, there is still a possibility to form a non-core−shell structure if the cation exchange is so fast that the rate of exchange becomes competitive with the precipitation rate of shell components, ending up with a non-core−shell structure. The core−shell architecture has been used widely as a method to improve the optical properties of nanoparticles. However, as discussed above, some may not be core−shell. This is not surprising because many characterization techniques are not able to show the non-core−shell structure. For instance, optical properties, such as lifetimes of emissive Ln^{3+} ions, can be improved not only by the core−shell structure but also simply by the increase of the size, which reduces surface quenching by decreasing the surface area and reduces concentration quenching by increasing the distance between Ln^{3+} ions, respectively.[25] The increase in size determined by TEM or other techniques does not prove a core−shell structure, although it is consistent with core−shell structures. In addition, the indistinguishable contrast between lanthanide salts with TEM does not provide direct information about the core−shell structure. On the other hand, cation exchange could be used as an alternative method to make core−shells by a partial cation exchange of surface layers. In addition, as shown by semiconductor nanomaterials, it could also be used as a method to make some nanomaterials that cannot be made directly. For instance, Ln_2O_3 (Ln = Er, Tm, Yb, and Lu) nanotubes have been prepared, but this synthesis did not work with other lanthanides.[34] In this case, cation exchange might result in nanotubes of other lanthanide oxides.

CONCLUSIONS

Cation exchange in lanthanide fluoride nanoparticles takes place quickly and reversibly by exposing nanoparticles to another lanthanide ion. A trend can be seen that the early lanthanide ions replace the late lanthanide ions in lanthanide fluoride nanoparticles with a relatively high extent of exchange as compared with the reverse. Experimental results suggest a small driving force, which is supported by the examination of the thermodynamic cycle. Due to the cation exchange, some core−shell nanoparticles in the literature may have different structures rather than a core−shell. On the other hand, cation exchange may be used as an alternative method to make core−shell and some nanomaterials that cannot be made directly.

EXPERIMENTAL SECTION

The lanthanide nitrate salts were purchased from Aldrich in the highest purity available (at least 99.9%). Ammonium hydroxide used is an aqueous solution of NH_3 with a concentration of 28.0−30.0 wt %. All the chemicals were used as received without further purification.

Synthesis of Citrate-Stabilized Nanoparticles. The solution of 2 g of citric acid in 35 mL of distilled water was adjusted with ammonium hydroxide to pH 5−6 and heated to 75 °C followed by the dropwise addition of the solution of 1.33 mmol $Ln(NO_3)_3$ (Ln = La, Nd, Eu, Gd, and Yb) in 2 mL of distilled water and the solution of 0.126 g of NaF (3 mmol) in 4 mL of distilled water consecutively. After stirring for 1 h, the nanoparticles were precipitated with *ca.* 50 mL of absolute ethanol and isolated with centrifuge at 4000 rpm for 3 min. The supernatant was poured off, followed by washing the residual with 15−20 mL of absolute ethanol and then isolation with centrifuge. This washing process was repeated three times. The final purified nanoparticles were dried under vacuum. All the nanoparticles are highly water-dispersible (50 mg nanoparticles can be dispersed in 1 mL of water to get clear dispersions like water).

Cation-Exchange Reaction. The solution of 1 g of citric acid in 25 mL of distilled water was adjusted with ammonium hydroxide to pH 5−6, which was heated up to 75 °C. The dispersion of 100 mg of citrate-stabilized LnF_3 nanoparticles was added, followed by the addition of the solution of 1.33 mmol $Ln'(NO_3)_3$ in 2 mL of water. (Please note that no extra F^- was added.) After 1 min, nanoparticles were precipitated with *ca.* 30 mL of absolute ethanol and isolated with centrifuge at 4000 rpm for 3 min. The supernatant was poured off followed by washing with 15−20 mL of absolute ethanol and then isolation with centrifuge. This washing process was repeated three times. The final purified nanoparticles were dried under vacuum. The same procedure was used for the reaction for 30 min. All the nanoparticles are highly water-dispersible (50 mg nanoparticles can be dispersed in 1 mL of water to get clear dispersion like water). Please note that Ln and Ln′ mean two different Ln^{3+} ions.

Powder X-ray Diffraction. Approximately 20 mg of a sample was gently stirred in an alumina mortar to break up lumps. The powdery samples of nanoparticles were smeared onto a zero-background holder using ethanol. Step-scan X-ray powder diffraction data were collected over the 2θ range 20−100° with Cr (30 kV, 15 mA) radiation on a Rigaku Miniflex diffractometer with variable divergence slit, 4.2° scattering slit, and 0.3 mm receiving slit. The scanning step size was 0.02° 2θ with a counting time of 6 s per step.

Transmission Electron Microscopy. High-resolution transmission electron microscopy was done with a Tecnai G2 field emission scanning transmission electron microscopy operated at 200 kV. The nanoparticle dispersion was dropcasted onto a carbon grid and allowed to dry in air at room temperature. The carbon grid with samples on it was then mounted into the vacuum sample chamber for imaging.

Energy Dispersive X-ray Spectroscopy. Energy dispersive X-ray spectroscopy was done using a Hitachi S-3500N scanning electron microscope, operated at 20 kV and a resolution of 102 eV. Dry powdered samples were attached to the substrate using a double-sided carbon tape and mounted onto the sample holder. The measurements were done on the basis of an assemble of nanoparticles. Three measurements were done for each sample to calculate standard deviations.

Fluorescence Studies. Fluorescence analyses were done using an Edinburgh Instruments FLS 920 fluorescence system, which was equipped with a 10 Hz Q-Switched Quantel Brilliant, pumped by a Nd:YAG laser, attached with an optical parametric oscillator with an optical range of 410−2400 nm as excitation source for lifetime measurements. A red-sensitive Peltier-cooled Hamamatsu R955 photomultiplier tube with a photon counting interface was used as a detector of Eu^{3+} emission. Lifetimes were measured by excitation at 464 nm and collection of the emission at 591 nm. All luminescence measurements were done with aqueous solutions of nanoparticles. Effective lifetimes were calculated using signal intensity greater than 1% of the maximum intensity with Origin 7.0 program based on the following equation:[35]

$$\tau_{eff} = \frac{\int_0^\infty tI(t)dt}{\int_0^\infty I(t)dt}$$

Acknowledgment. We gratefully acknowledge the generous funding from the Natural Science and Engineering Research Council (NSERC), the Canada Foundation for Innovation (CFI), and the British Columbia Knowledge Development Fund (BCKDF) of Canada.

Supporting Information Available: EDX spectra and calculation of solubility product This material is available free of charge *via* the Internet at http://pubs.acs.org.

REFERENCES AND NOTES

1. Son, D. H.; Hughes, S. M.; Yin, Y. D.; Alivisatos, A. P. Cation Exchange Reactions in Ionic Nanocrystals. *Science* **2004**, *306*, 1009–1012.
2. Zhu, W.; Wang, W. Z.; Shi, J. L. A Reverse Cation-Exchange Route to Hollow PbSe Nanospheres Evolving from Se/Ag_2Se Core/Shell Colloids. *J. Phys. Chem. B* **2006**, *110*, 9785–9790.
3. Robinson, R. D.; Sadtler, B.; Demchenko, D. O.; Erdonmez, C. K.; Wang, L. W.; Alivisatos, A. P. Spontaneous Superlattice Formation in Nanorods through Partial Cation Exchange. *Science* **2007**, *317*, 355–358.
4. Park, K. H.; Oh, S. J. Electron-Spectroscopy Study of Rare-Earth Trihalides. *Phys. Rev. B* **1993**, *48*, 14833–14842.
5. Jeong, U. Y.; Xia, Y. N.; Yin, Y. D. Large-Scale Synthesis of Single-Crystal CdSe Nanowires through a Cation-Exchange Route. *Chem. Phys. Lett.* **2005**, *416*, 246–250.
6. Camargo, P. H. C.; Lee, Y. H.; Jeong, U.; Zou, Z. Q.; Xia, Y. N. Cation Exchange: A Simple and Versatile Route to Inorganic Colloidal Spheres with the Same Size but Different Compositions and Properties. *Langmuir* **2007**, *23*, 2985–2992.
7. Jeong, U.; Kim, J. U.; Xia, Y. N. Monodispersed Spherical Colloids of Se@CdSe: Synthesis and Use as Building Blocks in Fabricating Photonic Crystals. *Nano Lett.* **2005**, *5*, 937–942.
8. Pietryga, J. M.; Werder, D. J.; Williams, D. J.; Casson, J. L.; Schaller, R. D.; Klimov, V. I.; Hollingsworth, J. A. Utilizing the Lability of Lead Selenide to Produce Heterostructured Nanocrystals with Bright, Stable Infrared Emission. *J. Am. Chem. Soc.* **2008**, *130*, 4879–4885.
9. Michalet, X.; Pinaud, F. F.; Bentolila, L. A.; Tsay, J. M.; Doose, S.; Li, J. J.; Sundaresan, G.; Wu, A. M.; Gambhir, S. S.; Weiss, S. Quantum Dots for Live Cells *In Vivo* Imaging, and Diagnostics. *Science* **2005**, *307*, 538–544.
10. Sivakumar, S.; Diamente, P. R.; van Veggel, F. C. J. M. Silica-Coated Ln^{3+}-Doped LaF_3 Nanoparticles as Robust Down- and Upconverting Biolabels. *Chem.—Eur. J.* **2006**, *12*, 5878–5884.
11. Chatteriee, D. K.; Rufalhah, A. J.; Zhang, Y. Upconversion Fluorescence Imaging of Cells and Small Animals Using Lanthanide Doped Nanocrystals. *Biomaterials* **2008**, *29*, 937–943.
12. Liu, Y. F.; Chen, W.; Wang, S. P.; Joly, A. G. Investigation of Water-Soluble X-ray Luminescence Nanoparticles for Photodynamic Activation. *Appl. Phys. Lett.* **2008**, *92*, 043901-1–043901-3.
13. Diamente, P. R.; Raudsepp, M.; van Veggel, F. C. J. M. Dispersible Tm^{3+}-Doped Nanoparticles that Exhibit Strong 1.47 μm Photoluminescence. *Adv. Funct. Mater.* **2007**, *17*, 363–368.
14. Sivakumar, S.; van Veggel, F. C. J. M.; Raudsepp, M. Bright White Light through Upconversion of a Single NIR Source from Sol−Gel-Derived Thin Film Made with Ln^{3+}-Doped LaF_3 Nanoparticles. *J. Am. Chem. Soc.* **2005**, *127*, 12464–12465.
15. Heer, S.; Lehmann, O.; Haase, M.; Güdel, H. U. Blue, Green, and Red Upconversion Emission from Lanthanide-Doped $LuPO_4$ and $YbPO_4$ Nanocrystals in a Transparent Colloidal Solution. *Angew. Chem., Int. Ed.* **2003**, *42*, 3179–3182.
16. Evanics, F.; Diamente, P. R.; van Veggel, F. C. J. M.; Stanisz, G. J.; Prosser, R. S. Water-Soluble GdF_3 and GdF_3/LaF_3 Nanoparticles-Physical Characterization and NMR Relaxation Properties. *Chem. Mater.* **2006**, *18*, 2499–2505.
17. Bridot, J. L.; Faure, A. C.; Laurent, S.; Riviere, C.; Billotey, C.; Hiba, B.; Janier, M.; Josserand, V.; Coll, J. L.; Vander Elst, L.; *et al.* Hybrid Gadolinium Oxide Nanoparticles: Multimodal Contrast Agents for *In Vivo* Imaging. *J. Am. Chem. Soc.* **2007**, *129*, 5076–5084.
18. Hifumi, H.; Yamaoka, S.; Tanimoto, A.; Citterio, D.; Suzuki, K. Gadolinium-Based Hybrid Nanoparticles as a Positive MR Contrast Agent. *J. Am. Chem. Soc.* **2006**, *128*, 15090–15091.
19. Stouwdam, J. W.; van Veggel, F. C. J. M. Near-Infrared Emission of Redispersible Er^{3+}, Nd^{3+}, and Ho^{3+} Doped LaF_3 Nanoparticles. *Nano Lett.* **2002**, *2*, 733–737.
20. Wang, X.; Zhuang, J.; Peng, Q.; Li, Y. D. A General Strategy for Nanocrystal Synthesis. *Nature* **2005**, *437*, 121–124.
21. Wang, Z. L.; Quan, Z. W.; Jia, P. Y.; Lin, C. K.; Luo, Y.; Chen, Y.; Fang, J.; Zhou, W.; O'Connor, C. J.; Lin, J. Facile Synthesis and Photoluminescent Properties of Redispersible CeF_3, CeF_3: Tb^{3+}, and CeF_3: Tb^{3+}/LaF_3 (Core/Shell) Nanoparticles. *Chem. Mater.* **2006**, *18*, 2030–2037.
22. Hantzschel, N.; Zhang, F. B.; Eckert, F.; Pich, A.; Winnik, M. A. Poly(*N*-vinylcaprolactam-*co*-glycidyl methacrylate) Aqueous Microgels Labeled with Fluorescent LaF_3: Eu Nanoparticles. *Langmuir* **2007**, *23*, 10793–10800.
23. Marcus, Y. *Ion Solvation*; John Wiley & Sons: Chichester, UK, 1985.
24. Dong, C.; Raudsepp, M.; van Veggel, F. C. J. M. Kinetically-Determined Crystal Structures of Undoped and La^{3+}-Doped LnF_3. *J. Phys. Chem. C* **2008**, In press.
25. Sudarsan, V.; van Veggel, F. C. J. M.; Herring, R. A.; Raudsepp, M. Surface Eu^{3+} Ions Are Different Than "Bulk" Eu^{3+} Ions in Crystalline Doped LaF_3 Nanoparticles. *J. Mater. Chem.* **2005**, *15*, 1332–1342.
26. Brixner, L. H.; Crawford, M. K.; Hyatt, G.; Carnall, W. T.; Blasse, G. Structure and Luminescence of the $La_{1-x}Gd_xF_3$ System. *J. Electrochem. Soc.* **1991**, *138*, 313–317.
27. Lide, D. R. *Handbook of Chemistry and Physics*; CRC Press: Boca Raton, FL, 1996.
28. Chan, E. M.; Marcus, M. A.; Fakra, S.; ElNaggar, M.; Mathies, R. A.; Alivisatos, A. P. Millisecond Kinetics of Nanocrystal Cation Exchange Using Microfluidic X-ray Absorption Spectroscopy. *J. Phys. Chem. A* **2007**, *111*, 12210–12215.
29. Leung, L. K.; Komplin, N. J.; Ellis, A. B.; Tabatabaie, N. Photoluminescence Studies of Silver-Exchanged Cadmium Selenide Crystals - Modification of a Chemical Sensor for

Aniline Derivatives by Heterojunction Formation. *J. Phys. Chem.* **1991**, *95*, 5918–5924.
30. Bulatov, V. L.; Grimes, R. W.; Harker, A. H. The Mobility of Ions in Lanthanum Fluoride Nanoclusters. *JOM-e* **1997**, *49*.
31. Moeller, T.; Martin, D. F.; Thompson, L. C.; Ferrüs, R.; Feistel, G. R.; Randall, W. J. Coordination Chemistry of Yttrium and Rare Earth Metal Ions. *Chem. Rev.* **1965**, *65*, 1–50.
32. Lezhnina, M. M.; Justel, T.; Katker, H.; Wiechert, D. U.; Kynast, U. H. Efficient Luminescence from Rare-Earth Fluoride Nanoparticles with Optically Functional Shells. *Adv. Funct. Mater.* **2006**, *16*, 935–942.
33. Li, C.; Liu, X.; Yang, P.; Zhang, C.; Lian, H.; Lin, J. LaF_3, CeF_3, CeF_3: Tb^{3+}, and CeF_3: Tb^{3+}@LaF_3 (Core−Shell) Nanoplates: Hydrothermal Synthesis and Luminescence Properties. *J. Phys. Chem. C* **2008**, *112*, 2904–2910.
34. Yada, M.; Mihara, M.; Mouri, S.; Kuroki, M.; Kijima, T. Rare Earth (Er, Tm, Yb, Lu) Oxide Nanotubes Templated by Dodecylsulfate Assemblies. *Adv. Mater.* **2002**, *14*, 309–313.
35. Shionoya, S.; Yen, W. M. *Phosphor Handbook*; CRC Press: Boca Raton, FL, 1999.